Thermodynamics, Transport, and Fluid Mechanics

Extension of the COSMO-UNIFAC Thermodynamic Model

Ruisong Zhu, Mohsen Taheri, Jie Zhang, and Zhigang Lei

Ind. Eng. Chem. Res., **Just Accepted Manuscript** • DOI: 10.1021/acs.iecr.9b05963 • Publication Date (Web): 06 Jan 2020

Extension of the COSMO-UNIFAC Thermodynamic Model

Ruisong Zhu, Mohsen Taheri, Jie Zhang,* and Zhigang Lei*

State Key Laboratory of Chemical Resource Engineering, Beijing University of Chemical Technology, Box 266, Beijing 100029, China

ABSTRACT: In this work, *a priori* COSMO-SAC model was combined with the original UNIFAC model, and thus the new COSMO-SAC-UNIFAC thermodynamic model with a strong predictive power for fluid phase equilibrium (VLE, LLE) was proposed. By this means the group binary parameter matrix of original UNIFAC model was extended by introducing the new 648 vacant parameter pairs for 51 main functional groups for the conventional substances in this work. Moreover, the combined thermodynamic model was first applied to process simulation on gas drying with ionic liquids (ILs). To verify the reliability of COSMO-SAC-UNIFAC model, the predictive values were directly compared with experimental data coming from this work, our previous work, and literature. The moderately accurate predictions of COSMO-SAC-UNIFAC model demonstrate the high potential applicability of this new model, especially for numerous systems with missing parameters including ILs which are normally encountered in the original UNIFAC model.

1. INTRODUCTION

Phase equilibrium data is crucial to the separation of mixtures in chemical production processes. For example, the gas drying process, which combines VLE (vapor-liquid equilibrium) and LLE (liquid-liquid equilibrium), has been studied by many researchers in recent years. The liquid absorbents are mainly triethylene glycol (TEG)[1] and ionic liquids (ILs).[2] In the actual production, process simulation plays an important role. To study fluids, researchers often predict their thermodynamic properties by thermodynamic models. Among others, the UNIFAC and COSMO-based models are common methods for predicting VLE and LLE.[3]

The UNIFAC model, based on the group contribution methods (GCMs),[4] is very popular amongst chemists and chemical engineers. In GCMs, chemical compounds are divided into the predefined functional groups. The activity coefficient (γ) of the mixture can be calculated through the group binary interaction parameters. Chemical compounds are more diverse and complex than functional groups and may contain new functional groups. Even more importantly, in the original UNIFAC model, for the existing groups, general researchers can't obtain the most recent group binary parameters except for parts of UNIFAC Consortium.[5] Thus, exhaustive experimental efforts are needed for completing the blank parameters.

The COSMO-based models contain two sub-models: COSMO-RS and COSMO-SAC. The former (COSMO for real solvents) proposed by Klam[6] has been embedded into the commercial software like COSMOtherm, while it is not an open access for general researchers yet. However, general researchers may have access to the latter (COSMO segment activity coefficient) first put forward by Lin.[7] The COSMO-SAC model can predict

the phase equilibrium based on quantum chemical calculations.[8] This method has been embedded into the famous commercial software like Aspen Plus.

The combined COSMO-UNIFAC model (i.e., COSMO-RS-UNIFAC and COSMO-SAC-UNIFAC) was first reported by Prof. Lei in our previous work[9] for extending the UNIFAC group parameter matrix. It has the following unique advantages: (1) providing the moderately accurate prediction; (2) being independent of any experimental data, and thus avoiding the consumption of manpower, material, time, and cost; (3) having a simple fitting procedure and a fast calculation speed; and (4) its parameters being easily input into the commercial simulation packages like Aspen Plus, PROII, and ADF (Amsterdam Density Functional) for process simulation.

In our previous work, we found that the COSMO-SAC model has the similar predictive capacity as COSMO-RS model, but it is free access to public.[9] So in this work, the original UNIFAC model was further combined with COSMO-SAC model and extended to estimate the VLE and LLE. For the conventional substances, more than 600 new group binary parameters were introduced. The applicability of COSMO-SAC-UNIFAC model was tested by comparing the original UNIFAC, COSMO-SAC, and COSMO-SAC-UNIFAC models.

2. EXPERIMENTAL SECTION

2.1. Materials. Chloromethane (CH_3Cl), H_2O, and 1-ethyl-3-methyl-imidazolium tetrafluoroborate ([EMIM][BF_4]) are used here. [EMIM][BF_4] was put in a vacuum oven and dried for three hours at 120 ℃ for the subsequent experiment. Then, Karl Fischer titration were used for determine the moisture in IL. Supporting Information “Specifications of Materials” provides more details.

2.2. Instruments and Procedures.

2.2.1. VLE Experiment.

The experimental work on measuring the VLE data was carried out using a modified equilibrium apparatus. The schematic graph of experimental device is depicted in Supporting Information Figure S1. Our previous work[10] described more details on the design and reliability of this experimental apparatus.

2.2.2. Chloromethane (CH_3Cl) Gas Dehydration Experiment with ILs.

For gas dehydration experiment, Supporting Information Figure S2 provides the information on apparatus, flow sheet, specifications and types of all equipment. The gas dehydration process mainly includes an absorption column, a liquid pump, a gas moisture analyzer, and vacuum drying cabinet. A liquid pump was used for delivering the dried IL to the top of absorption column. The CH_3Cl feed gas passed through the saturated water and entered into the absorption column at the bottom. The moisture of CH_3Cl gas product leaving from the top of absorption column could be detected by the moisture analyzer. The used IL flowed out from the bottom and then was recovered by vacuum drying cabinet.

3. COMPUTIONAL DETAILS

3.1. COSMO-SAC Model.

The COSMO-SAC model can estimate the thermodynamic properties with quantitative calculation method independent of any experimental data, which is somewhat different from the UNIFAC model. In this work, the temperature range was set from 273.15 to 393.15 K and activity coefficients at infinite dilution (γ^{∞}) were estimated by the COSMO-SAC model (the ADF version 2018.105 with the COSMO-SAC version 2013). Herein, the parameters in

COSMO-SAC calculation were derived from Xiong et al.' work.[11] The reliability of estimated infinite dilution activity coefficients was evaluated by

$$\mathrm{ARD}_{\gamma^{\infty}} = \frac{1}{N}\sum_{i=1}^{N}\left|\frac{\gamma_{i,\mathrm{cal}}^{\infty} - \gamma_{i,\mathrm{COSMO\text{-}SAC}}^{\infty}}{\gamma_{i,\mathrm{COSMO\text{-}SAC}}^{\infty}}\right| \quad (1)$$

The fitting results as well as the corresponding average relative deviations (ARDs) are listed in Supporting Information Tables S1-S18.

3.2. UNIFAC Model.

The UNIFAC model is a popular predictive model based on the regression of experimental data (empirical). Fitting γ^{∞} coming from the COSMO-SAC model can get the missing group binary parameters. The activity coefficient estimated in the UNIFAC model has two parts: one is the combinatorial activity coefficient ($\ln\gamma_i^{\mathrm{C}}$), which reflects the influence of molecular sizes and shapes; the other is the residual activity coefficient ($\ln\gamma_i^{\mathrm{R}}$), which reflects the intermolecular interaction energies. $\ln\gamma_i^{\mathrm{R}}$ includes the group binary interaction parameters between two different groups defined as a_{nm} and a_{mn}. Supporting Information "UNIFAC model" and Table S19 provide more information on the UNIFAC model.

3.3. COSMO-SAC-UNIFAC Model.

A combination of COSMO-SAC and UNIFAC models produces a new predictive COSMO-SAC-UNIFAC model. Even if the a_{nm} and a_{mn} in the original UNIFAC model are missing, it can still be used to predict the data of VLE and LLE. For COSMO-SAC-UNIFAC model, the previously existing parameters in the original UNIFAC model do not need to be changed. Moreover, the numerous vacant parameters can be filled with new parameters obtained in this work. That is, γ^{∞} values obtained from the COSMO-SAC model (version

2013 Xiong[11]) were input as "artificial values" into the UNIFAC model, and the regression was conducted within the Aspen Plus framework (version 8.4). For example, the compound N,N-dimethylformamide is considered as a whole group named DMF, while nitrobenzene is considered to make up of ACH and $ACNO_2$. Thus, for the N,N-dimethylformamide - nitrobenzene system, the a_{nm} and a_{mn} of DMF/ACH, DMF/$ACNO_2$, and ACH/$ACNO_2$ are concerned. However, the interaction parameters between DMF and $ACNO_2$ are not available in literature, whereas other parameters (between DMF and ACH and between ACH and $ACNO_2$) are adopted as in the original UNIFAC model. In this case, the COSMO-SAC model was applied to compute the γ^{∞} values to regress the missing group binary interaction parameters (between DMF and $ACNO_2$). That is, these values already present in the UNIFAC model were import into Aspen Plus, and the missing group binary interaction parameters were regressed through selecting the function "Regression". These new parameters together with the previously existing parameters are all used for the estimation of phase equilibrium of the N,N-dimethylformamide-nitrobenzene system. More details on fitting procedure can be found in Supporting Information.

To prove the applicability of COSMO-SAC-UNIFAC model, the predictive values of VLE and LLE were compared with experimental data. In the case of VLE, the average relative deviations for pressure (ARD$_P$) and activity coefficient (ARDγ) are respectively defined as

$$\mathrm{ARD}_P = \frac{1}{N}\sum_{i=1}^{N}\left|\frac{P_{i,\mathrm{cal}} - P_{i,\mathrm{exp}}}{P_{i,\mathrm{exp}}}\right| \tag{2}$$

$$\mathrm{ARD}_\gamma = \frac{1}{N}\sum_{i=1}^{N}\left|\frac{\gamma_{i,\mathrm{cal}} - \gamma_{i,\mathrm{exp}}}{\gamma_{i,\mathrm{exp}}}\right| \tag{3}$$

where $P_{i,\mathrm{cal}}$ and $\gamma_{i,\mathrm{cal}}$ represent the COSMO-SAC-UNIFAC calculated pressures and activity coefficients, respectively; $P_{i,\mathrm{exp}}$ and $\gamma_{i,\mathrm{exp}}$ represent the experimental data. For LLE, the average relative deviations for composition (ARD_C) between experimental data and the calculated values by COSMO-SAC-UNIFAC model including binary and ternary systems are defined as

$$\mathrm{ARD}_C = \frac{1}{4m}\sum_{i=1}^{1}\sum_{j=1}^{2}\sum_{k=1}^{m}\left|\frac{x_{ijk,cal}-x_{ijk,exp}}{x_{ijk,exp}}\right| \tag{4}$$

$$\mathrm{ARD}_C = \frac{1}{4m}\sum_{i=1}^{2}\sum_{j=1}^{2}\sum_{k=1}^{m}\left|\frac{x_{ijk,cal}-x_{ijk,exp}}{x_{ijk,exp}}\right| \tag{5}$$

where $x_{ijk,cal}$ and $x_{ijk,exp}$ (mole fraction) represent the calculated and experimental liquid compositions, respectively, and m is the number of data points (see Supporting Information Tables S21-S38 for more details).

For the CH_3Cl + water + [EMIM][BF_4] system, [EMIM][BF_4] is made up of one [MIM][BF_4] group and one CH_3 group (see Supporting Information Figure S3). All the group binary parameters concerned are regressed in the similar manner as mentioned above and the results are listed in Table 1. The average relative deviation for water content in gas product is defined as

$$\mathrm{ARD}_y = \frac{1}{m}\sum_{i=1}^{m}\left|\frac{y_{i,cal}-y_{i,exp}}{y_{i,exp}}\right| \tag{6}$$

where $y_{i,cal}$ and $y_{i,exp}$ represent the calculated and experimental water contents (mass fraction), respectively.

4. RESULTS AND DISCUSSION

The COSMO-SAC-UNIFAC parameters matrix is shown in Supporting Information Figure S4. This matrix includes 648 new group binary parameters calculated by the

COSMO-SAC-UNIFAC model for conventional substances (excluding ILs).

4.1. Vapor-Liquid Equilibrium.

4.1.1. The Systems with the UNIFAC Model Parameters Already Available.

In the case that the UNIFAC model parameters are already available, such as the ethyl alcohol-water system, the COSMO-SAC-UNIFAC model group binary parameters are consistent with those of UNIFAC model. As shown in Figure 1, the prediction of UNIFAC model overlaps with that of COSMO-SAC-UNIFAC model, both of them giving moderately accurate prediction. However, the COSMO-SAC model gives the worst accuracy compared to experimental data. For more details, please see Supporting Information Table S21.

4.1.2. The Systems with Only Part of the UNIFAC Model Parameters Available.

In general, the prediction accuracy decreases with the increase of the vacancy parameters of UNIFAC model. For the phenol + N-methylacetamide, chlorobenzene + furfuran, N,N-dimethylformamide (DMF) + nitrobenzene, and methoxyethanol + dimethylsulfoxide systems, the missing interaction parameters account for 33.3% of all the required ones, which is higher than 20% for the chlorobenzene - benzaldehyde system. In this case, the COSMO-SAC-UNIFAC model is more accurate than the original UNIFAC model because the missing parameters are taken on as zero as usual (see Figure 2). Moreover, as shown in Figure 2(a), the original UNIFAC model even cannot correctly estimate the azeotropic phenomenon for the phenol (1) + N-methylacetamide (2) azeotropic system.

Moreover, the ARDs of COSMO-SAC model are significantly higher than those of COSMO-SAC-UNIFAC, although it could predict the rough trends. Overall, the COSMO-SAC-UNIFAC model can give the best prediction. More details can be found in

Supporting Information Tables S24-S28.

4.1.3. The Systems with All the UNIFAC Model Parameters Not Available.

When all the UNIFAC model parameters can not be available, the group binary parameters have to be derived by the combination of COSMO-SAC and UNIFAC models. Figure 3 shows the predictions for VLE of the UNIFAC, COSMO-SAC, and COSMO-SAC-UNIFAC models as well as the experimental data for four systems (i.e., methanol + N-methyl-2-pyrrolidone (NMP), morpholine + acetonitrile, DMF + pyridine, and NMP + 1,2-dichloroethane) (see Supporting Information Tables S30-S34). It seems that the higher the proportion of missing parameters in the original UNIFAC model, the worse the predictive accuracy. Evidently, the COSMO-SAC-UNIFAC model outperforms both the UNIFAC and COSMO-SAC models.

When it comes to the NMP + 1,2-dichloroethane system (see Figure 3(c)), the ARD of UNIFAC model reaches as high as 93.42%, which is more than triple the ARD of COSMO-SAC-UNIFAC model. Figure 3(d) shows that although the COSMO-SAC model could roughly predict the trends in most cases, opposite VLE trend even arises.

4.2. Liquid-Liquid Equilibrium.

4.2.1. Binary LLE.

In liquid-liquid extraction, The LLE data on the aromatics + glycols systems are needed for process simulation and design. Unfortunately, the group binary interaction parameters between chlorobenzene and 1,2-ethanediol and between nitrobenzene and 1,2-ethanediol are missing in the current UNIFAC model. As shown in Figure 4, the COSMO-SAC-UNIFAC model is the best, while the COSMO-SAC model performs worst. The COSMO-SAC model

could not even predict the phase splitting (see Figure 4(b)). More details can be found in Supporting Information Tables S35-S36.

4.2.2. Ternary LLE.

In chemical industry, extractive distillation is often used to separate the components with similar boiling points. The process requires the addition of a solvent (or entrainer) that could change the relative volatility of key components.[22] The solvent may form a vapor-liquid-liquid equilibrium system with the components to be separated in distillation column. Thus, LLE data are also essential for both chemical equipment design and practical unit operations like extractive distillation and liquid-liquid extraction.

The LLE for two ternary systems (i.e., morpholine + acetonitrile + octane and cyclohexane + 1,2-dichloroethane + DMSO) were estimated by the UNIFAC, COSMO-SAC, and COSMO-SAC-UNIFAC models (more information can be found in Supporting Information Tables S37-S38). As shown in Figure 5, the predicted values by COSMO-SAC-UNIFAC model are closer to the experimental data than those of the other two models. It agrees well for LLE at the low x_1 concentration. In particular, the ARDs for COSMO-SAC model are even more than 100% in some cases. Although its prediction almost lies on the experimental tie lines, a little large deviation from the experimental binodal curves arises.

4.3. Comparison among the UNIFAC, COSMO-SAC, and COSMO-SAC-UNIFAC Models.

The VLE, saturated vapor pressure and LLE for 16 binary and 2 ternary systems were calculated by the UNIFAC, COSMO-SAC, and COSMO-SAC-UNIFAC models, and

compared with experimental data. As summarized in Table 2, the predictive accuracy of COSMO-SAC-UNIFAC model is better than that of the other two models as a whole, exhibiting the closer predictions to experimental data, i.e., "1 + 1 ≥ 2". Thus, the applicability of COSMO-SAC-UNIFAC model is further validated in this work.

4.4. Process Simulation Using the COSMO-SAC-UNIFAC Model.

In this work, the COSMO-SAC-UNIFAC model was further applied to process simulation with the CH_3Cl gas dehydration process as an example. The gas dehydration experiment was performed with [EMIM][BF_4] as absorbent under normal temperature and pressure. The moisture contents of CH_3Cl gas and IL were 2150 ppm (mass fraction) and 500 ppm (mass fraction), respectively. In the experiment, the flowrate of CH_3Cl was kept at a constant value of 500 mL·minute^{-1}, while the flowrate of IL was variable. In the absorption column, CH_3Cl gas entered from the bottom of absorption column, while the IL fed from the top. Process simulation under experimental condition was made using the UNIFAC, COSMO-SAC, and COSMO-SAC-UNIFAC models within the Aspen Plus (version 8.4) framework. The effect of volume flowrate of IL (VIL) on the moisture content in CH_3Cl gas product (y_1, mass fraction) is shown in Figure 6. It can be seen that y_1 first decreases sharply and then tends to be stable with the increase of V_{IL}. Moreover, the COSMO-SAC-UNIFAC model prediction is the closest to experimental data. Supporting Information Table S41 provides the experiment data as well as the predicted values by these models.

We further scaled up the CH_3Cl gas dehydration process to the industrial scale, and used the COSMO-SAC-UNIFAC model to simulate and optimize the process. The CH_3Cl feed gas with the moisture 4650 ppm (mass fraction) and the flowrate 4000 kg·h^{-1} is required to

reduce the moisture below 200 ppm. As depicted in Figure 7, this process includes one gas absorption column, one flash drum, one pump, and several heat exchangers and coolers.

To achieve the better separation performance, design and operating parameters were optimized by sensitivity analysis. For absorption column, it is evident that the number of theoretical plates (N_i), the temperature of absorption column (T_a) and the mass flowrate of IL (M_{IL}) are important parameters. As shown in Figures 8(a) and (b), the increase of M_{IL} leads to the decrease of y_1, M_{IL} = 3000 kg·h^{-1} being the turning point. Moreover, the more the N_i, the lower the y_1. Four theoretical plates suffice for meeting the separation requirement, and y_1 increases with the increase of T_a. In addition, flash tank for the recovery of IL is another main equipment in the dehydration process. Its operating temperature (T_f) and pressure (P_f) can significantly influence y_1. Among these factors, increasing temperature and reducing pressure are beneficial to decreasing y_1 (see Figures 8(c) and (d)). Therefore, the final optimum conditions are determined as follows: N_i = 4, M_{IL} = 3000 kg·h^{-1}, T_a = 20 ℃, T_f = 120 ℃, and P_f = 0.03 atm. For more details on operating conditions and simulation results, please see Supporting Information Tables S39-S41.

5. CONCLUSIONS

In this work, 651 vacant parameter pairs were obtained in the COSMO-SAC-UNIFAC model parameter matrix so that more chemical thermodynamic systems can be predicted effectively and efficiently using this proposed model. The COSMO-SAC-UNIFAC model can give comparatively more accurate prediction of VLE and LLE when compared to the original UNIFAC and COSMO-SAC models. Furthermore, the COSMO-SAC-UNIFAC model was first applied to process simulation on the CH_3Cl gas dehydration with IL at either

laboratory or industrial scale, demonstrating the reliability of the COSMO-SAC-UNIFAC model for the predictions of systems including ILs. In the end, we are pleased to announce that the COSMO-SAC-UNIFAC model will be embedded into such famous commercial softwares as ADF and ASPEN Plus in the coming 2020/2021 releases.

■ ASSOCIATED CONTENT

Supporting Information

There is free SI on the ACS Publications website.

Details on the apparatus, experimental data, fitting procedure, parameters, COSMO-SAC-UNIFAC model parameter matrix, and simulated results of all three models mentioned in the paragraph can be obtained from online version (xls).

■ AUTHOR INFORMATION

Corresponding Author

*Phone: +86-10-64433695; E-mail: zhangjie@mail.buct.edu.cn (J. Zhang).

E-mail: leizhg@mail.buct.edu.cn (Z. Lei).

ORCID

Jie Zhang: 0000-0002-3059-1978

Zhigang Lei: 0000-0001-7838-7207

Notes

The authors declare no competing financial interest.

■ ACKNOWLEDGMENTS

This work is financially supported by the National Natural Science Foundation of China under Grant (No. U1862103).

■ REFERENCES

(1) Kong, Z.; Mahmoud, A.; Liu, S. A Parametric Study of Different Recycling Configurations for the Natural Gas Dehydration Process Via Absorption Using Triethylene Glycol. *Process Integra. Optimiz. Sustain.* **2018**, *2*, 447-460.

(2) Yu G; Jiang Y.; Lei Z. Pentafluoroethane Dehydration with Ionic Liquids. *Ind. Eng. Chem. Res*. **2018**, *57*, 12225-12234.

(3) Lin, S.; Wang, L.; Chen, W. Prediction of miscibility gaps in water/ether mixtures using COSMO-SAC model. *Fluid Phase Equilib*. **2011**, *310*, 19-24.

(4) Gmehling, J. Present status of group-contribution methods for the synthesis and design of chemical processes. *Fluid Phase Equilib*. **1998**, *144*, 37-47.

(5) Wittig, R.; Lohmann, J.; Gmehling, J. Vapor-liquid Equilibria by UNIFAC Group Contribution. 6. Revision and Extension. *Ind. Eng. Chem. Res*. **2003**, *42*, 183-188.

(6) Klamt, A. Conductor-like Screening Model for Real Solvents: A New Approach to the Quantitative Calculation of Solvation Phenomena. *J. Phys. Chem*. **1995**, *99*, 2224-2235.

(7) Lin, S.; Sandler, S. I. A Priori Phase Equilibrium Prediction from a Segment Contribution Solvation Model. *Ind. Eng. Chem. Res*. **2002**, *41*, 899-913.

(8) Li, X.; Siddique, F.; Silva, G. T. Quantum chemical evidence for the origin of the red/blue colors of hydrangea macrophylla sepals. *New J. Chem.* **2019**, *43*, 32-24.

(9) Dong, Y.; Zhu, R.; Guo, Y.; Lei, Z. A United Chemical Thermodynamic Model: COSMO-UNIFAC. *Ind. Eng. Chem. Res*. **2018**, *57*, 15954-15958.

(10) Han, J.; Lei, Z.; Dai, C.; Li, J. Vapor pressure measurements for binary mixtures containing ionic liquid and predictions by the conductor-like screening model for real solvents. *J. Chem. Eng. Data* **2016**, *61*, 1117-1124.

(11) Xiong, R.; Sandler, S.; Russell, I. An improvement to COSMO-SAC for predicting thermodynamic properties. *Ind. Eng. Chem. Res*. **2014**, *53*, 8265-8278.

(12) Lei, Z.; Dai, C.; Liu, X.; Xiao, L.; Chen, B. Extension of the UNIFAC model for ionic liquids. *Ind. Eng. Chem. Res*.**2012**, *51*, 12135-12144.

(13) Kai, F.; Michael, H.; Oliver, A.; Martin, P.; Jurgen, G. Vapor-Liquid Equilibria and Enthalpies of Mixing for Binary Mixtures of N-Methylacetamide with Aniline, Decane, Ethylene Glycol, Naphthalene, Phenol, and Water. *J. Chem. Eng. Data* **1997**, *42*, 875-881.

(14) Chen, C.; Zhou, F.; Xu, C. Measurement and Correlation of Isobaric Vapor–Liquid Equilibrium of Three Binary Systems Containing Chlorobenzene at 50.00 and 101.33 kPa. *Trans. Tianjin Univ.* **2018**, *24*, 8-15.

(15) Prasad, T.; Singh, S.; Ahmed, P.; Millikarjun, G.; Reddy, P. L.; Prasad, D. H. L. Excess Gibbs energies of binary mixtures formed by nitrobenzene with selected compounds at 94.95 kPa. *Fluid Phase Equilib.* **2007**, *252*, 53-56.

(16) Zhao, S.; Bai, P.; Sun, C. Isobaric vapor-liquid equilibrium for binary and ternary systems with toluene, 2-methoxyethanol and dimethyl sulfoxide at 101.3 kPa. *Fluid Phase Equilib*. **2014**, *375*, 37-44.

(17) Riechert, O.; Zeiner, T.; Sadowski, G. Phase Equilibria in Systems of Morpholine, Acetonitrile, and n-Alkanes. *J. Chem. Eng. Data* **2015**, *60*, 2098-2103.

(18) Liu, M.; Xu, J.; Fang, X.; Xia, S. Vapor-liquid equilibria for the binary system of pyridine-dimethylformamide. *J. Chem. Eng. Chinese Univ.* **1989**, *3*, 33-38.

(19) Gnanakumari, P.; Rao, M.; Prasad, D.; Kumar, Y. Vapor-Liquid Equilibria and Excess Molar Enthalpies for N-Methyl-2-pyrrolidone with Chloroethanes and Chloroethenes. *J. Chem. Eng. Data* **2003**, *48*, 535-540.

(20) Rehak, K.; Dreiseitlova, J. Binary liquid-liquid equilibrium in the systems containing monofunctional benzene derivates and 1,2-ethanediol. *Fluid Phase Equilib*. **2006**, *249*, 104-108.

(21) Gao, X.; Yang, Z.; Xia, S. Liquid–liquid equilibrium data for binary systems containing o-dichlorobenzene and nitrobenzene. *Fluid Phase Equilib*. **2015**, *385*, 175-181.

(22) Lim, K. J. A. ; Cabajar, A. A. ; Lobarbio, C. F. Y. Extraction of bioactive compounds from mango (mangifera indica l. var. carabao) seed kernel with ethanol–water binary solvent systems. *J. Food Sci. Technol.* **2019**, *56*, 2536-2544.

(23) Riechert, O.; Zeiner, T.; Sadowski, G. Phase Equilibria in Systems of Morpholine, Acetonitrile, and n-Alkanes. *J. Chem. Eng. Data* **2015**, *60*, 2098-2103.

(24) Cele, N.; Bahadur, I.; Redhi, G.; Ebenso, E. (Liquid + liquid) equilibria measurements for ternary systems (sulfolane + a carboxylic acid + n-heptane) at T = 303.15 K and at 0.1 MPa. *J. Chem. Thermodyn*. **2016**, *96*, 169-174.

Table Caption

Table 1. Group Binary Interaction Parameters for the CH_3Cl, IL, and H_2O System in the COSMO-SAC-UNIFAC Model.

Table 2. Average Relative Deviations (ARD_γ, ARD_P, and ARD_C) for All Models Concerned in This Work.

Table 1. Group Binary Interaction Parameters for the CH_3Cl, IL, and H_2O System in the COSMO-SAC-UNIFAC Model

m	*n*	α_{mn}	α_{nm}
CH_3Cl	CH_3	61.13[b]	-11.12[b]
CH_3Cl	H_2O	986.50[b]	156.40[b]
CH_3Cl	$[MIM]BF_4$	697.20[b]	16.51[b]
CH_3	H_2O	1318.00	300.00
CH_3	$[MIM]BF_4$	1333.00[a]	275.80[a]

[a]Parameters coming from literature;[12] [b]Parameters coming from this work; Others are from Aspen Plus database (version 8.4).

Table 2. Average Relative Deviations (ARD_γ, ARD_P, and ARD_C) for All Models Concerned in This Work

Systems	Specific ARDs	COSMO-SAC	UNIFAC	COSMO-SAC-UNIFAC
(1). The systems with the UNIFAC model parameters already available				
ethanol + water	ARD_γ	0.0847	0.0002	0.0002
(2). All the UNIFAC model parameters not available				
HF + H_2O	ARD_γ	1.1657	20.8661	0.3145
methanol + NMP	ARD_P	1.3252	0.3189	0.1747
DMF + pyridine	ARD_γ	0.0426	0.1101	0.0412
morpholine + acetonitrile	ARD_γ	0.5544	0.2416	0.4146
NMP + dichloroethane	ARD_γ	0.3389	0.9342	0.2633
(3). Only part of the UNIFAC model parameters available				
methanol + DMAC	ARD_P	1.8562	0.1562	0.0352
acetic acid + NMP	ARD_γ	0.2149	0.6267	0.1734
DMS + ethanol	ARD_γ	0.1222	0.3278	0.1198
phenol + N-methylacetamide	ARD_P	2.8155	0.2330	0.1100
chlorobenzene + benzaldehyde	ARD_γ	0.1381	0.1603	0.0610
chlorobenzene + Furfural	ARD_γ	0.0371	0.1029	0.0561
DMF + nitrobenzene	ARD_γ	0.0441	0.1566	0.0509
2-methoxyethanol + DMSO	ARD_γ	0.0288	0.2642	0.1339
chlorobenzene + 1,2-ethanediol	ARD_C	2.3325	0.0788	0.0588
nitrobenzene + 1,2-ethanediol	ARD_C	0.9562	0.0886	0.0630
sulfolane + butanoic acidh + heptane	ARD_C	1.5720	0.2896	0.2836
morpholine + acetonitrile + octane	ARD_C	0.2040	0.1220	0.0469
Total	ARD_P	5.9969	0.7081	0.3199
	ARD_γ	2.7715	23.7907	1.6289
	ARD_C	5.0647	0.5790	0.4523

Figure Captions

Figure 1. VLE of the ethanol (1) + H_2O (2) system. —, predictions of the COSMO-SAC model; - - -, predictions of the original UNIFAC model; —, predictions of the COSMO-SAC-UNIFAC model; ■, experimental values.

Figure 2. VLE of the (a) phenol (1) + N-methylacetamide (2), (b) chlorobenzene (1) + benzaldehyde (2), (c) chlorobenzene (1) + furfuran (2), (d) N,N-dimethylformamide (1) + nitrobenzene (2), and (e) 2-ethoxyethanol (1) + dimethyl sulfoxide (2) systems. —, predictions of the COSMO-SAC model; - - -, predictions of the original UNIFAC model; —, predictions of the COSMO-SAC-UNIFAC model; ■, experimental data.[13-16] The experimental data points come from refs 14 (Copyright 2017 Tianjin University and GmbH Germany Springer), 15 (Copyright 2007 Elsevier B.V.), and 16 (Copyright 2014 Elsevier B.V.) with permissions.

Figure 3. VLE of the (a) methanol (1) + NMP (2), (b) morpholine (1) + acetonitrile (2), (c) DMF (1) + pyridine (2), and (d) N-methyl-2-pyrrolidone (1) + 1,2-dichloroethane (2) systems. —, predictions of the COSMO-SAC model; - - -, predictions of the original UNIFAC model; —, predictions of the COSMO-SAC-UNIFAC model; ■, experimental data.[17-19] The experimental data points come from ref 18 (Copyright 1989 China National Knowledge Infrastructure (CNKI)) with permission.

Figure 4. LLE of the (a) chlorobenzene (1) + 1,2-ethanediol (2) and (b) nitrobenzene (1) + 1,2-ethanediol (2) systems. —, predictions of the original UNIFAC model; —, predictions of the COSMO-SAC-UNIFAC model; ---, predictions of the COSMO-SAC model; ●, predictions of the original UNIFAC model; ▲, predictions of the COSMO-SAC-UNIFAC model; ★, predictions of the COSMO-SAC model; ■, experimental data.[20-21] The experimental data points come from refs 20 (Copyright 2006 Elsevier B.V.) and 21 (Copyright 2014 Elsevier B.V.) with permissions.

Figure 5. LLE of the (a) sulfolane (1) + butanoic acid (2) + heptane (3), (b) morpholine (1) + acetonitrile (2) + octane (3). —, experimental tie line; ●, predictions of the original UNIFAC model; ▲, predictions of the COSMO-SAC-UNIFAC model; ★, predictions of the COSMO-SAC model; ■, experimental data.[23,24] The experimental data points come from ref 24 (Copyright 2016 Elsevier B.V.) with permission.

Figure 6. Water content in the CH_3Cl gas product. —, predictions of the COSMO-SAC model; —, predictions of the original UNIFAC model; —, predictions of the COSMO-SAC-UNIFAC model; ■, experimental data measured in this work.

Figure 7. CH_3Cl gas dehydration process with the IL [EMIM][BF_4] as absorbent at industrial scale.

Figure 8. Effect of M_{IL} (a), T_a (b), T_f (c), and P_f (d) on water content in the CH_3Cl gas product. ---, targeted water content. (a) T_a = 20 ℃, P_a = 0.1 MPa, T_f = 120 ℃, P_f = 0.03 atm; (b) P_a = 0.1 MPa, $N_{i,}$ = 4, M_{IL} = 4000 kg·h^{-1}, T_f = 120 ℃, P_f = 0.03 atm; (c) T_a = 20 ℃, P_a = 0.1 MPa, N_i = 4, M_{IL} = 4000 kg·h^{-1}, P_f = 0.03 atm; (d) T_a = 20 ℃, P_a = 0.1 MPa, N_i = 4, M_{IL} = 4000 kg·h^{-1}, T_f = 120 ℃.

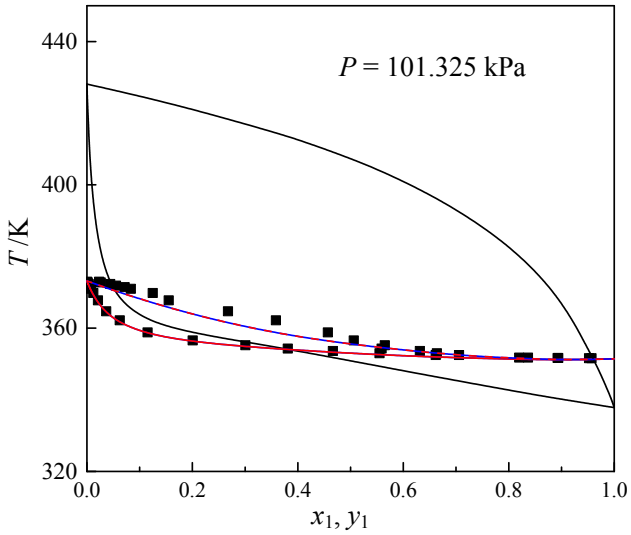

Figure 1. VLE of the ethanol (1) + H_2O (2) system. —, predictions of the COSMO-SAC model; - - -, predictions of the original UNIFAC model; —, predictions of the COSMO-SAC-UNIFAC model; ■, experimental values.

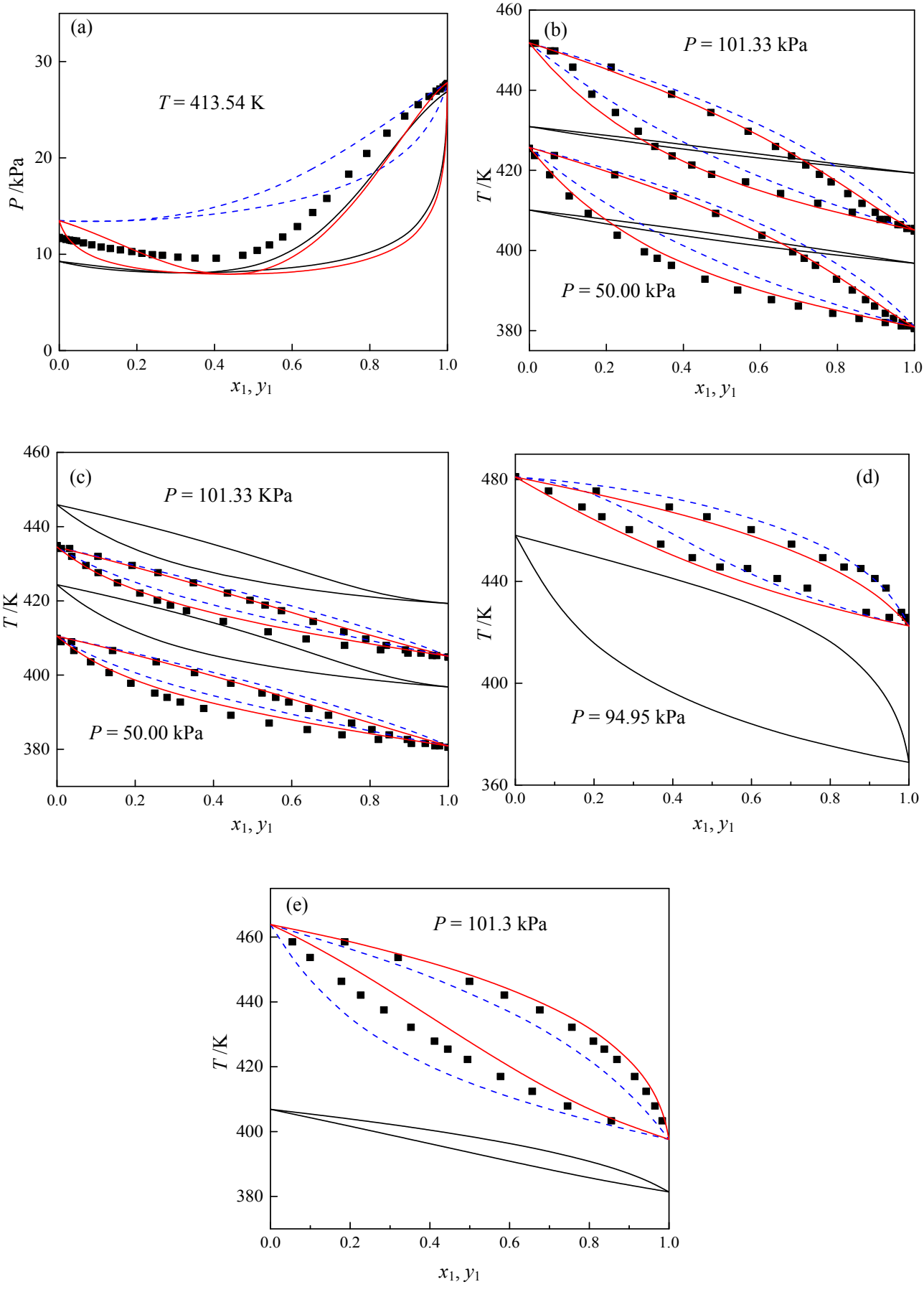
(a)
T = 413.54 K
P /kPa
x1, y1
(b)
P = 101.33 kPa
P = 50.00 kPa
T /K
x1, y1
(c)
P = 101.33 KPa
P = 50.00 kPa
T /K
x1, y1
(d)
P = 94.95 kPa
T /K
x1, y1
(e)
P = 101.3 kPa
T /K
x1, y1

Figure 2. VLE of the (a) phenol (1) + N-methylacetamide (2), (b) chlorobenzene (1) + benzaldehyde (2), (c) chlorobenzene (1) + furfuran (2), (d) N,N-dimethylformamide (1) + nitrobenzene (2), and (e) 2-ethoxyethanol (1) + dimethyl sulfoxide (2) systems. —, predictions of the COSMO-SAC model; - - -, predictions of the original UNIFAC model; —, predictions of the COSMO-SAC-UNIFAC model; ■, experimental data.[13-16] The experimental data points come from refs 14 (Copyright 2017 Tianjin University and GmbH Germany Springer), 15 (Copyright 2007 Elsevier B.V.), and 16 (Copyright 2014 Elsevier B.V.) with permissions.

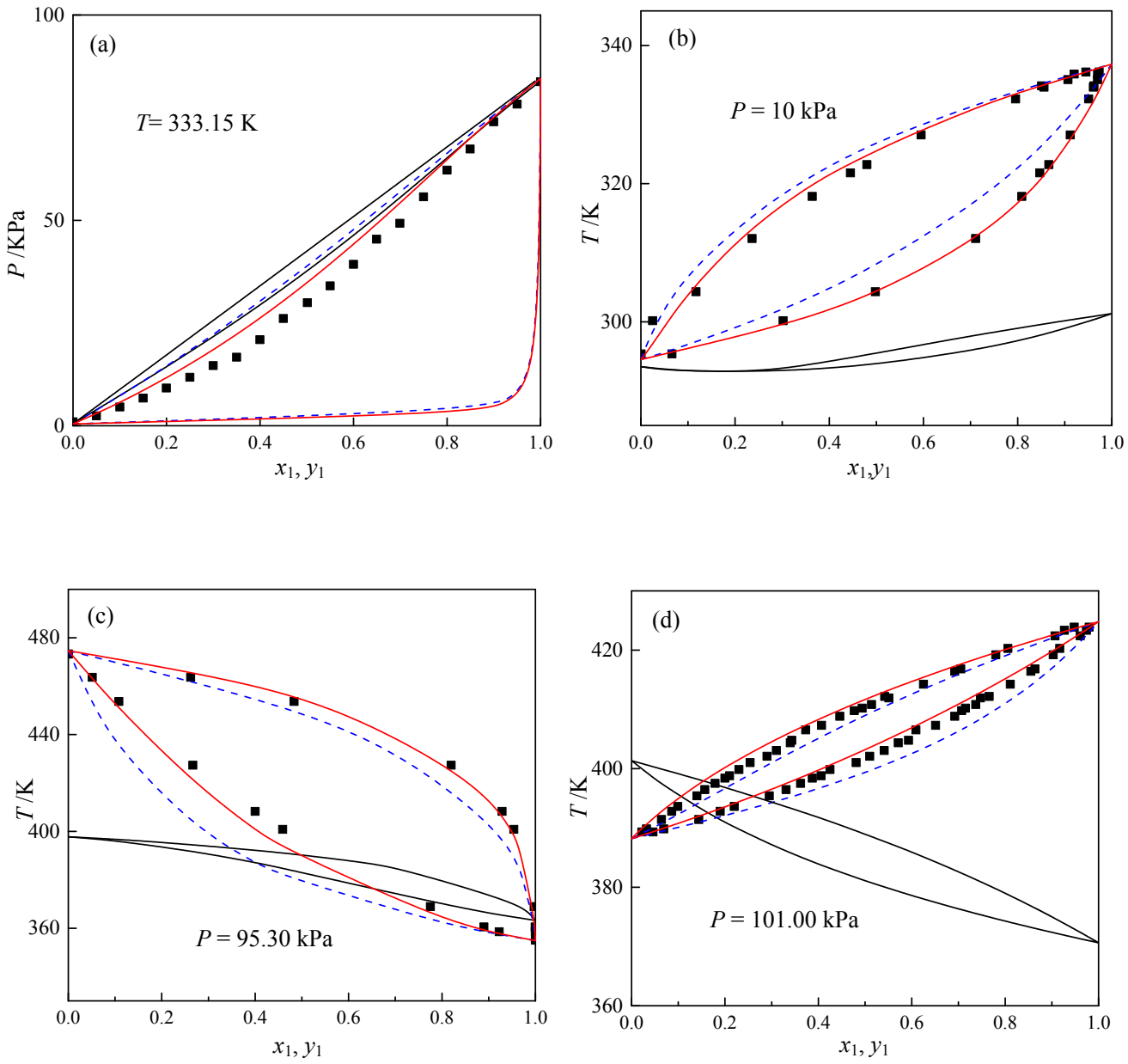

Figure 3. VLE of the (a) methanol (1) + NMP (2), (b) morpholine (1) + acetonitrile (2), (c) DMF (1) + pyridine (2), and (d) N-methyl-2-pyrrolidone (1) + 1,2-dichloroethane (2) systems. —, predictions of the COSMO-SAC model; - - -, predictions of the original UNIFAC model; —, predictions of the COSMO-SAC-UNIFAC model; ■, experimental data.[17-19] The experimental data points come from ref 18 (Copyright 1989 China National Knowledge Infrastructure (CNKI)) with permission.

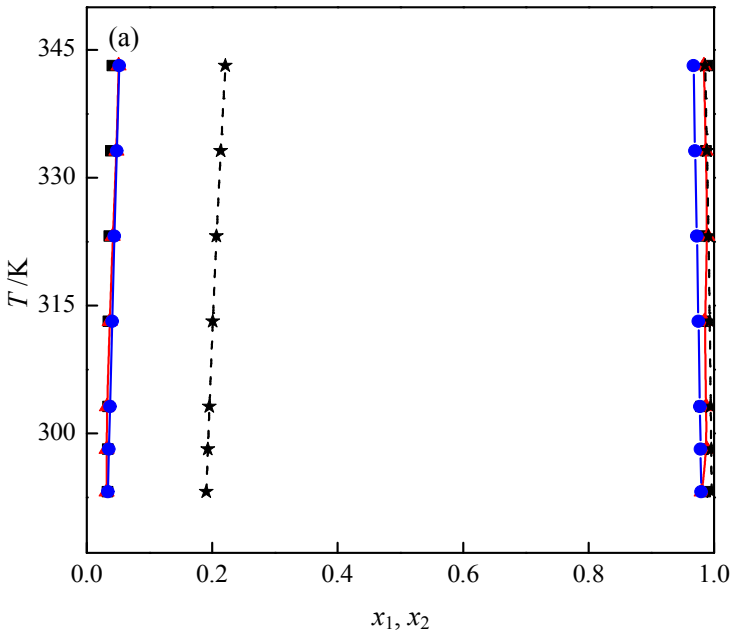
(a)
345
330
315
300
T /K
0.0
0.2
0.4
0.6
0.8
1.0
x1, x2

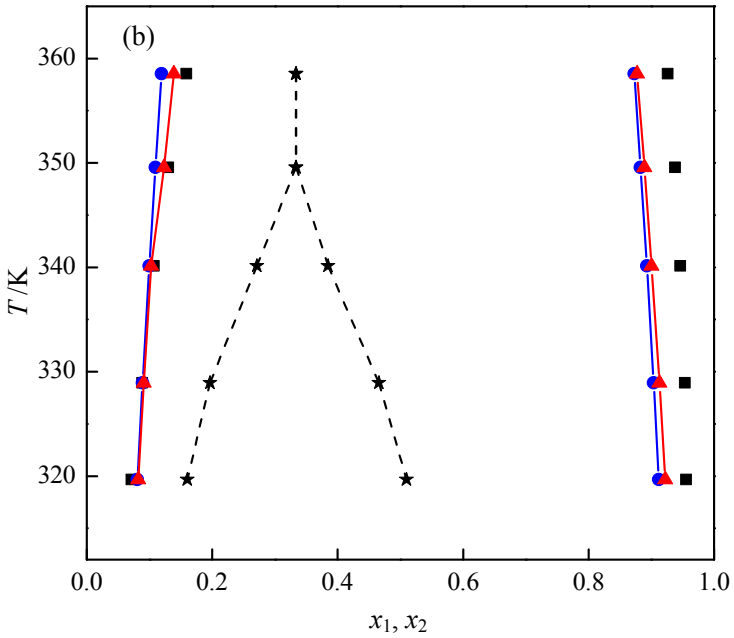
(b)
360
350
340
330
320
T /K
0.0
0.2
0.4
0.6
0.8
1.0
x1, x2

Figure 4. LLE of the (a) chlorobenzene (1) + 1,2-ethanediol (2) and (b) nitrobenzene (1) + 1,2-ethanediol (2) systems. —, predictions of the original UNIFAC model; —, predictions of the COSMO-SAC-UNIFAC model; - - -, predictions of the COSMO-SAC model; ●, predictions of the original UNIFAC model; ▲, predictions of the COSMO-SAC-UNIFAC model; ★, predictions of the COSMO-SAC model; ■, experimental data.[20-21] The experimental data points come from refs 20 (Copyright 2006 Elsevier B.V.) and 21 (Copyright 2014 Elsevier B.V.) with permissions.

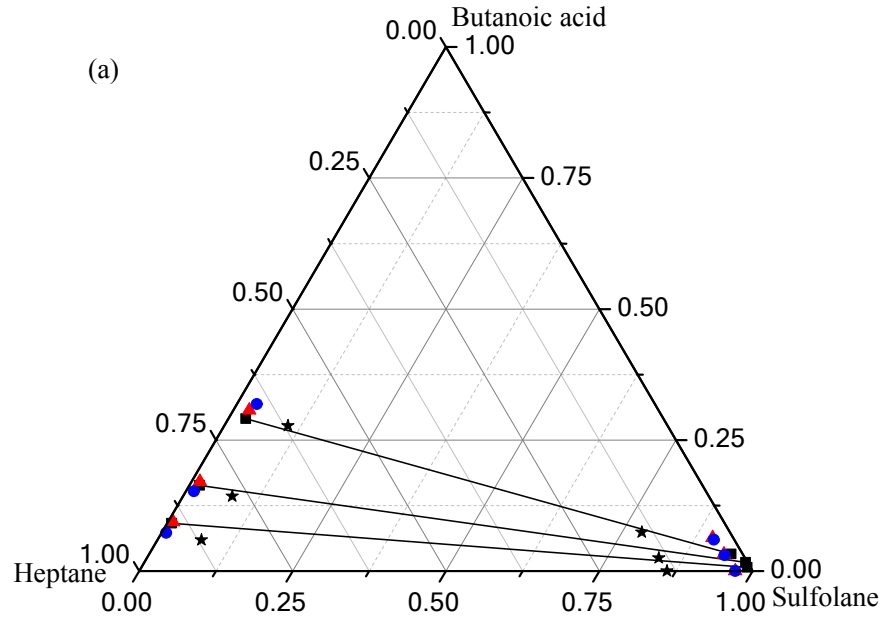
(a)
Butanoic acid
0.00
1.00
0.25
0.75
0.50
0.50
0.75
0.25
1.00
0.00
Heptane
Sulfolane
0.00
0.25
0.50
0.75
1.00

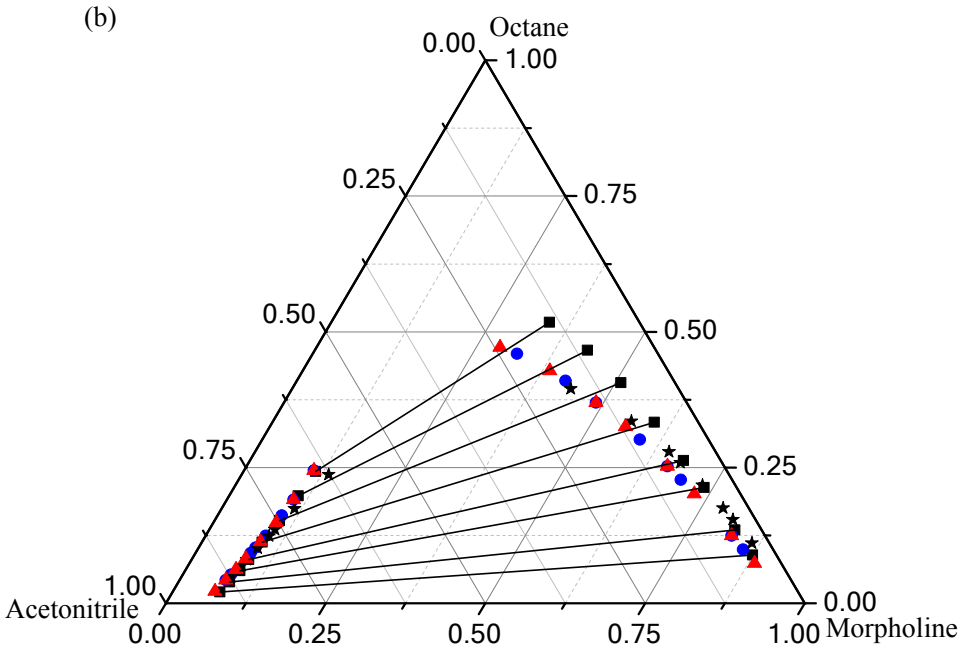
(b)
Octane
0.00
1.00
0.25
0.75
0.50
0.50
0.75
0.25
1.00
0.00
Acetonitrile
Morpholine
0.00
0.25
0.50
0.75
1.00

Figure 5. LLE of the (a) sulfolane (1) + butanoic acid (2) + heptane (3), (b) morpholine (1) + acetonitrile (2) + octane (3). —, experimental tie line; ●, predictions of the original UNIFAC model; ▲, predictions of the COSMO-SAC-UNIFAC model; ★, predictions of the COSMO-SAC model; ■, experimental data.[23,24] The experimental data points come from ref 24 (Copyright 2016 Elsevier B.V.) with permission.

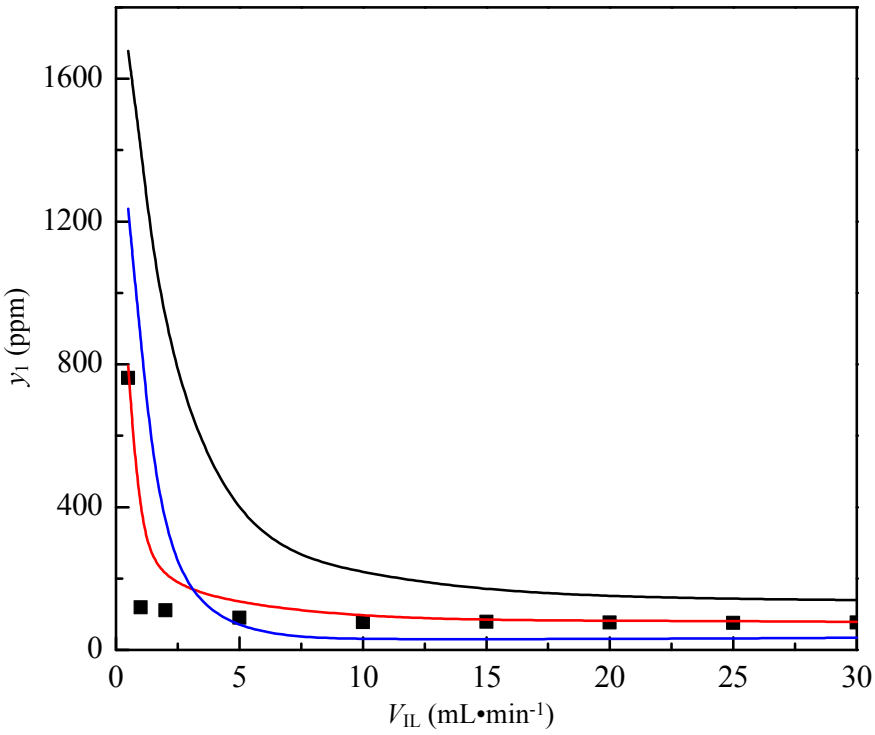

Figure 6. Water content in the CH_3Cl gas product. —, predictions of the COSMO-SAC model; —, predictions of the original UNIFAC model; —, predictions of the COSMO-SAC-UNIFAC model; ■, experimental data measured in this work.

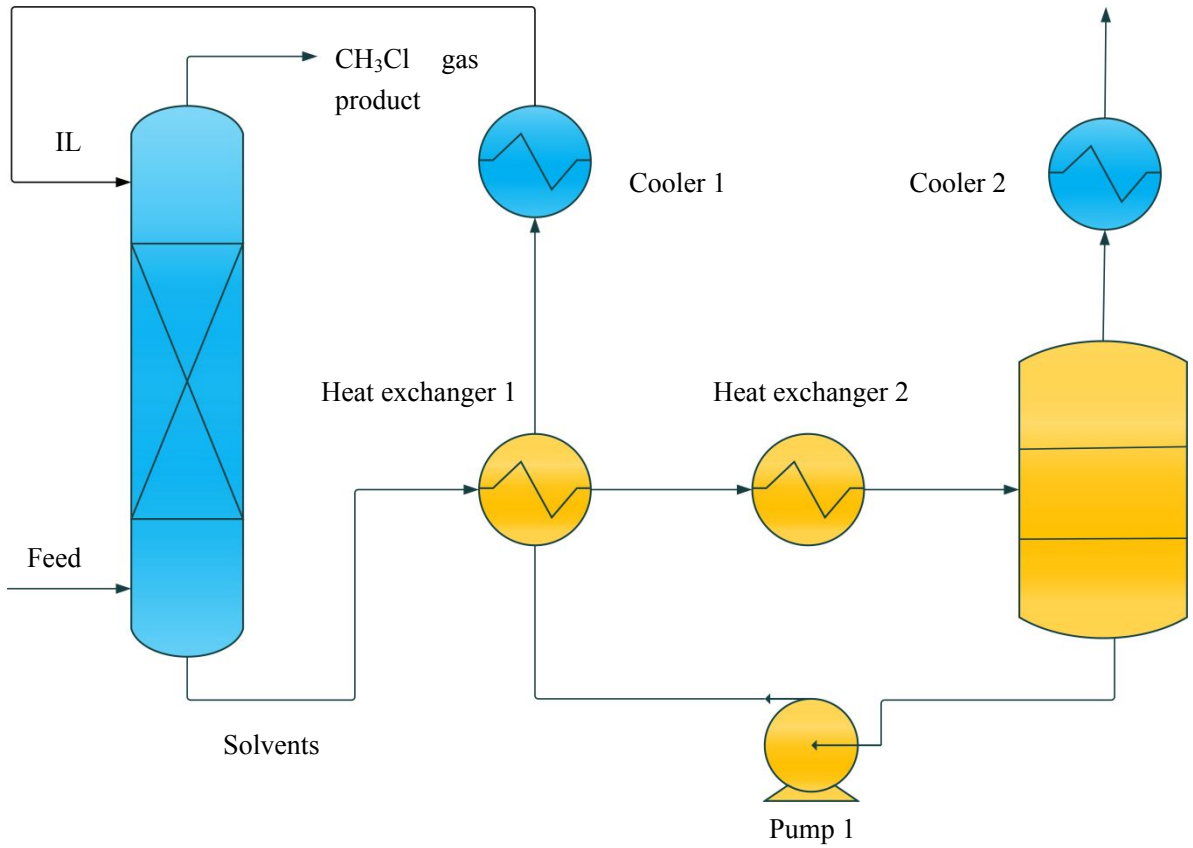

Figure 7. CH_3Cl gas dehydration process with the IL [EMIM][BF_4] as absorbent at industrial scale.

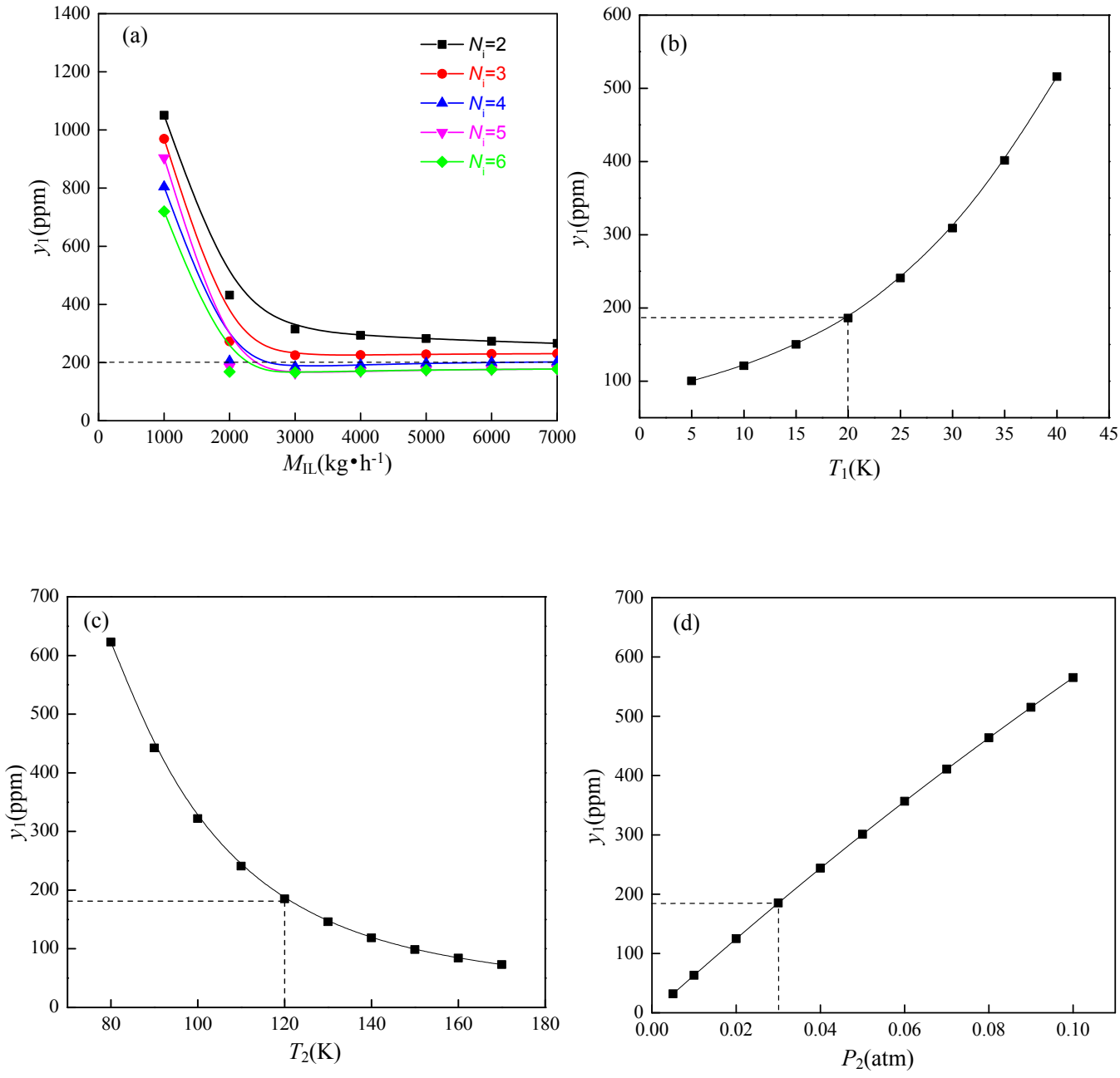

Figure 8. Effect of M_{IL} (a), T_a (b), T_f (c), and P_f (d) on water content in the CH_3Cl gas product. ---, targeted water content. (a) T_a = 20 ℃, P_a = 0.1 MPa, T_f = 120 ℃, P_f = 0.03 atm; (b) P_a = 0.1 MPa, $N_{i,}$ = 4, M_{IL} = 4000 kg·h^{-1}, T_f = 120 ℃, P_f = 0.03 atm; (c) T_a = 20 ℃, P_a = 0.1 MPa, N_i = 4, M_{IL} = 4000 kg·h^{-1}, P_f = 0.03 atm; (d) T_a = 20 ℃, P_a = 0.1 MPa, N_i = 4, M_{IL} = 4000 kg·h^{-1}, T_f = 120 ℃.

Table of Content (TOC) Graphic